Science Arts & Métiers (SAM)

is an open access repository that collects the work of Arts et Métiers Institute of Technology researchers and makes it freely available over the web where possible.

This is an author-deposited version published in: https://sam.ensam.eu
Handle ID: .http://hdl.handle.net/10985/11941

To cite this version :

Elisabeth MASSONI, Dorian DEPRIESTER - Submicrocristalline structure and dynamic recovery of cold flowformed ELI grade Ti-6Al-4V - In: ESAFORM, France, 2013-04-22 - Key Engineering Materials - 2013

Any correspondence concerning this service should be sent to the repository
Administrator : scienceouverte@ensam.eu

ResearchGate

See discussions, stats, and author profiles for this publication at: https://www.researchgate.net/publication/272047423

Submicrocristalline Structure and Dynamic Recovery of Cold Flowformed ELI Grade Ti-6Al-4V

Article *in* Key Engineering Materials · June 2013

DOI: 10.4028/www.scientific.net/KEM.554-557.157

CITATION
1

READS
30

2 authors, including:

Dorian Depriester
Ecole Nationale Supérieure d'Arts et Métiers
7 PUBLICATIONS **18** CITATIONS
SEE PROFILE

Some of the authors of this publication are also working on these related projects:

Project
Fluoti Project View project

All content following this page was uploaded by Dorian Depriester on 02 June 2015.

The user has requested enhancement of the downloaded file. All in-text references underlined in blue are added to the original document and are linked to publications on ResearchGate, letting you access and read them immediately.

Key Engineering Materials Vols 554-557 (2013) pp 157-168
© (2013) Trans Tech Publications, Switzerland
doi:10.4028/www.scientific.net/KEM.554-557.157
Online: 2013-06-13

Submicrocristalline structure and dynamic recovery of cold flowformed ELI grade Ti-6Al-4V

Dorian Depriester[1,a], and Elisabeth Massoni[1,b]

MINES ParisTech, Centre de Mise en Forme des matériaux (CEMEF), 1 rue Claude Daunesse CS 10207, France

[a]dorian.depriester@mines-paristech.fr, [b]elisabeth.massoni@mines-paristech.fr

Keywords: Ti-6Al-4V, ELI grade, dynamic recrystallization, cold flowforming, submicrocristallinne structure

Abstract. Flowforming is a means to produce seamless tubes by plastic deformation at room temperature. It consists in reducing the thickness of a tubular part mounted on a mandrel by deforming it using several rollers translating along the tube axis, while the tube is rotating along its axis. Thanks to the high compressive stresses, and to the incremental nature of the deformation process, flowforming can lead to a high thickness reduction and thus to high elongation of the deformed tubes.

Ti-6Al-4V (Extra Low Interstitial grade) tubes have been deformed by cold flowforming, with a thickness reduction ratio higher than 60%, and their microstructures have been investigated using light optical microscopy (LOM), scanning electron microscopy (SEM) and electron backscattered diffraction (EBSD). Based on EBSD data, a post-processing analysis has been performed in order to study the texture of the flowformed parts.

Optical Microscopy showed that the material could be deformed without displaying flow instability such as adiabatic shear banding, despite the fact that it has been processed out of the stable processing maps (high strain rate and low temperature). It also evidenced a major deformation along the tube axis accompanied with a slight twist due to torsion stress. EBSD analysis indicated the occurrence of continuous dynamic recrystallization, which is rarely reported in the α-β domain of such alloys. The recovery/ recrystallization effects resulted in a submicrocrystalline equiaxed structure, which is consistent with that previously reported for Ti-6Al-4V subjected to severe plastic deformation (SPD). The texture of the hexagonal α-phase appeared to be similar to that obtained on extruded Ti-6Al-4V, with a basal component perpendicular to the tube axis.

Introduction

Ti-6Al-4V mechanical behaviour. Ti-6Al-4V (Ti64) is an α-β titanium alloy and one of the most widely used light material for aerospace and aviation industry, due to its high strength, high corrosion resistance and low specific weight. In mill-annealed condition, this alloy is composed by about 95% of hexagonal close-packed (hcp) phase, denoted α phase, and balanced body-centred cubic (bcc) phase, denoted β phase. The so-called commercial (or standard) grade has an amount of oxygen content about 0.2 wt.%, mainly dispersed in interstitial sites. Those interstitial elements highly reduce the ductility of the α phase [1,2]. Thus, the extra-low interstitial (ELI) grade, with about 0.13 wt.% oxygen content, exhibits a better ductility than the commercial grade [3].

Because of the large proportion of the α phase, the macroscopic behaviour of the Ti64 is usually considered to be dominated by that of the α phase. Nevertheless, the Ti64 behaviour is quite different from that of commercial purity (CP) titanium in the α domain. Indeed, the lack of slip systems in the hcp structure and the high critical resolved shear stress (CRSS) for slip systems with a $< c >$ component [4] are compensated by several twinning modes, leading to a large ductility usually observed on CP titanium, even at room temperature [5,6]. On the contrary, it has been stated that the presence of both substitutional and interstitial elements, like Al, suppress the twinning activity [7]. As a result, even in ELI grade, Ti64 has a poor ductility in the α-β domain, especially at room temperature [3,8,9].

All rights reserved. No part of contents of this paper may be reproduced or transmitted in any form or by any means without the written permission of Trans Tech Publications, www.ttp.net. (ID: 147.171.83.252-14/04/15,09:07:18)

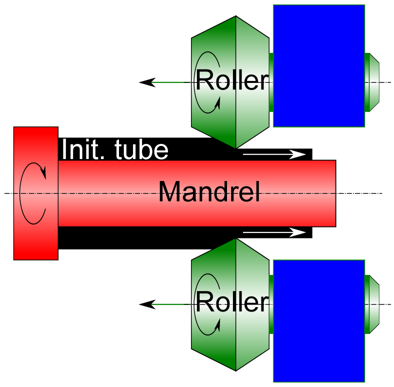

Fig. 1: Schematic view of backward flowforming. White and black arrows denote the longitudinal flow of the deformed material (coloured in black) and the roller feed, respectively.

Because of its poor conductivity, Ti64 deformed in the α-β domain is often subjected to adiabatic shear banding (ASB), leading to a localisation of the deformation and an important temperature rise in these bands [10,3,8]. According to those works, in α-β domain, ASB appears to occur for strain rate down to 1 s^{-1}. Hence, ASB is another critical limitation for cold forming of Ti64.

On the other side, superplastic behaviour has been numerously reported for Ti64 [11,12] and other α-β titanium alloys [13] below the β transus at very low strain rate and warm temperature. This behaviour is only reported with submiscrocrystalline structures (SMC), usually obtained by severe plastic deformation (SPD) [14-15], isothermal forging [11] or by protium treatment [12]. This superplastic behaviour has been related to the grain boundary sliding (GBS) phenomenon, requiring a low dislocation density and high angle grain boundaries (HAGBs) [15]. But such structures are hard to obtain and the necessary low strain rate for GBS is not compatible with industrial forming.

In the β range, the Ti64 alloy is much more ductile, especially at low strain rates (lower than 10^{-2} s^{-1}) because dynamic recrystallization (DRX) occurs [10,8,3] in that domain. To the best of the author's knowledge, the occurrence of DRX or dynamic recovery (DRV) on Ti64 deformed in the α-β domain using conventional tests (tensile, compressive and torsion tests) have been reported only by [16] at low strain rate (10^{-3} s^{-1}) and warm temperature (600 °C and 800 °C) .

Flowforming process. Flowforming (also called tube spinning) is a chipless production method to deform an initially tubular part, by reducing its wall thickness and then to elongate it. As depicted on figure 1, flowforming involves several free rollers (usually three) which translate along the axis of the initial tube mounted on a mandrel. The mandrel is rotating with that tube while the rollers are progressively reducing the thickness of the tube. In so-called backward flowforming, the material elongates on the opposite direction from the roller feed, as white and black arrows indicate on figure 1.

While several materials are widely used for cold flowforming, such as aluminium alloys [17,18] and low carbon steel [19,20], a few authors have reported a successful Ti64 flowforming [9,21]. Starting from a lamellar-structured ELI grade Ti64, using transmission electron microscopy (TEM), they stated that flowforming resulted in two types of α grains: long thin grains with high dislocation density and small equiaxed grains with low dislocation density. The second type have been attributed by the authors to DRV/DRX. But this phenomenon may be due to the lamellar structure, which is known to undergo the globularization phenomenon [8,22,16].

[9,21] have produced tubes utilizing different means (β extrusion, α-β extrusion, rotary piercing and flowforming) and extensively studied the mechanical properties of those tubes. They concluded that the flowforming process was the best candidate to improve yield stress, ultimate tensile stress and fatigue properties together without any remarkable decrease in ductility. Those improvements are related to the grain refinement and the DRV/DRX phenomenon observed by the authors, as discussed above.

Objectives. This objectives of this work are to report observations about the structure and the texture of a cold-flowformed Ti64, and to investigate the deformation mechanisms induced by that process, which lead to unusual ductility.

Experimental

Material. Ti64 ELI grade have been used for this study, the starting material was provided by Timet UK Ltd. The as-received material is produced by rod rolling, followed by mill-annealing. Then, the initial tube has been manufactured by core drilling. Microstrucure of the starting material, as illustrated on figure 2, is mainly equiaxed, with a few transformed β grains, consisting on thick α and β lamellae. Mean α-grain size is about 10 μm.

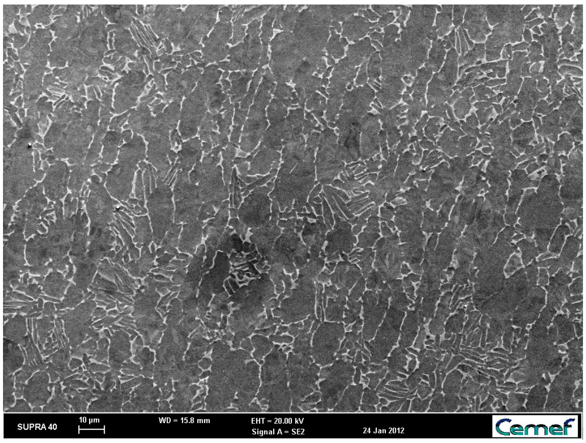

Fig. 2: Backscattered electron image (BSE) of the starting material

Processing. Two tubular preforms have been successfully backward-flowformed by Roxel company, with a 60 and 64% thickness reduction respectively, in a single pass each. No external heat source has been used (starting material at room temperature). Photographs of the flowformed tubes are depicted on figure 3. The change in color is a result of oxidation, evidencing the high temperature during the forming, due to plastic power and friction between the surface of the tubes and the tools, despite the very high lubrication (water based semi-synthetic coolant).

Microstructural characterization. For each tube (including the preform) optical micrographs were made along three orthogonal planes (longitudinal, transverse and tangential). On each part, one other specimen had been extracted along the longitudinal section for scanning electron microscopy (SEM) and electron backscattered diffraction analysis (EBSD). All the specimens were first prepared by sawing and then ground to 4000 grit, followed by diamond suspension (5 μm, 3 μm and 1 μm) polishing and finally 0.05 μm -silica suspension polishing. Specimen for optical microscopy were etched using the Kroll's reagent (10%HF+20%HNO_3 in water).

Optical micrographs were made using an Olympus PMG-3 inverted metallograph microscope with Nomarski filter and polarized light. FEG-SEM Zeiss Supra 40 operating at 20 kV, equipped with a backscattered electron detector (BSE) and Quantax CrystAlign EBSD system were utilized to investigate the grain structures and the textures of the deformed specimens. EBSD sampling points were spaced down to 19 nm, depending on the map.

(a) 60% reduction in thickness

(b) 64% reduction in thickness

Fig. 3: Photographs of the flowformed tubes investigated in this paper. Tails (on the left) are the non flowformed ends.

Results

Optical microscopy. Optical micrographs made from the deformed material can be seen on figure 4. The prior α grains, surrounded by β phase, can easily be identified. First, one may notice that the grains are severely elongated along the longitudinal direction (e_z). This result is consistent with the macroscopic deformation, mainly visible on the elongation of the tubes. Second, grain shape in the tangential planes (figures 4b and 4d) shows not only a deformation along e_z, but also a small deformation along the tangential direction (e_θ), creating a certain helix angle. This angle appears to decrease when the reduction ratio increases. This fact tends to demonstrate that the higher the reduction ratio, the more flowforming looks like extrusion (elongation along the roller feed direction *i.e.* axial); on the contrary, the lower the reduction ratio, the more flowforming looks like rolling (elongation along rolling direction *i.e.* tangential).

Due to very high lubrication during the flowforming processing, the material is quenched just after deformation. Yet, there is no evidence of transformed β grains, indicating that the temperature has not probably exceeded the β transus (around 980 °C for ELI grade). According to this statement, all the deformation is processed in the α-β domain. Nevertheless, there is no evidence of ASB on the micrographs of the figure 4 despite the moderate strain rate (around $10\,s^{-1}$). The fact that no ASB occurs may be due to the rotational symmetry, which is inconsistent with the ASB kinematic.

SEM observations. Utilizing the backscattered electron detector, single orientation (sub)grains can be distinguished, depending on there gray scale. BSE images on the longitudinal section of the flowformed tubes are presented on figure 5. It appears that the prior α phase has been fragmented into very small individual cells, which can be identified as grains or subgrains. Those cells are equiaxed and have a sub-micrometer scale (as illustrating on figure 5b : 100 to 300 nm size). Those results are consistent with those obtained by SPD [11,14,15].

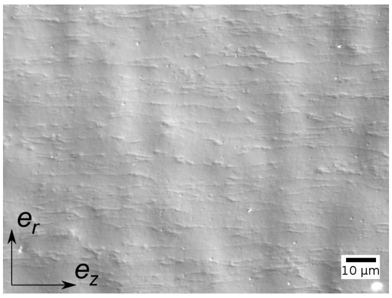

(a) 60% : longitudinal section

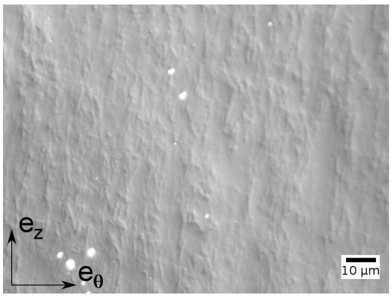

(b) 60% : tangential section

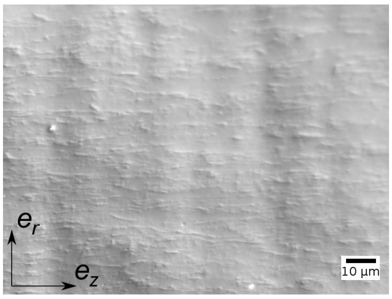

(c) 64% : longitudinal section

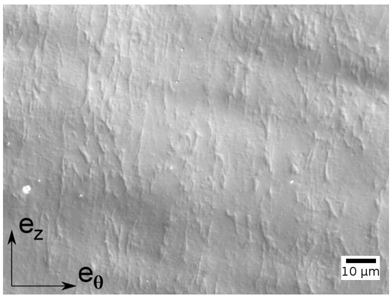

(d) 64% : tangential section

Fig. 4: Optical micrographs of the material deformed with 60% and 64% reduction in thickness

As illustrated on figure 5b, no cell can be identified in the β phase, reflecting the absence of rearrangement of the dislocations, and hence no recovery-like effect.

EBSD study. In order to characterize the boundaries between the cells, an EBSD analysis has been performed on the longitudinal sections of the deformed material. One may notice that this analysis is quite hard to do on those samples, considering the high dislocation density, which drastically degrades the Kikuchi patterns required for the analysis. [**?**] have managed to perform that analysis on flowformed Ti64 only after a stress-relief treatment, which slightly reduces the misorientation within the grains. The high resolution EBSD system used in the present work permitted to scan valuable maps. The orientation maps obtained by the EBSD analysis are depicted on figure 6. On that figure, black zone indicates non indexed points, which can be suspected to correspond with high dislocation density grains or grains/subgrains boundaries. The equiaxed cells identified on BSE images can be recognized on orientation maps. The β phase has almost not been indexed at all, probably due to a too high crystalline defects (like dislocations), which is consistent with the BSE observations (fig. 5), on which no internal β cell were identified.

On the 60%-flowformed material (fig. 6a), three kinds of grains can be identified:

I. long thin grains with moderate interganular misorienation, which correspond to medium dislocation density

II. small equiaxed grains, with low dislocation density

III. high dislocation density grains, presented as ``black zones'' on orientation maps, appearing equiaxed on these maps.

The I-type grain seems absent on the 64%-flowformed material, suggesting that it corresponds to the first stage of the deformation. Figure 6c plots the misorientation profile from the first point along the segments (A) and (B) on map 6b. Both curves display some plateaus, separated by low angle boundaries (LAGBs), as depicted on curve (A), or HAGBs, as depicted on curve (B). The first is typical of sub-grains, whereas the second is typical of grains. Those statements suggest the occurrence of both DRV and DRX during flowfomring, as already reported by [21].

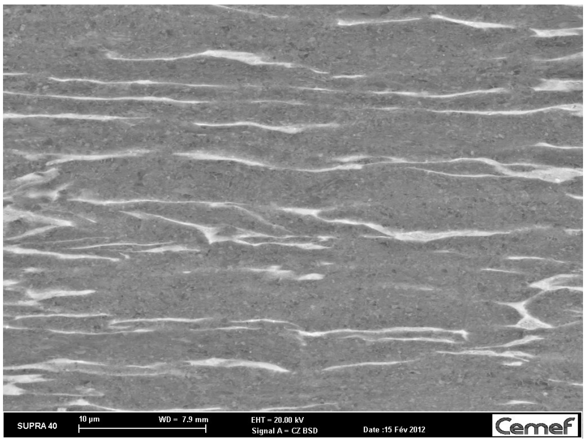

(a) ×2 000

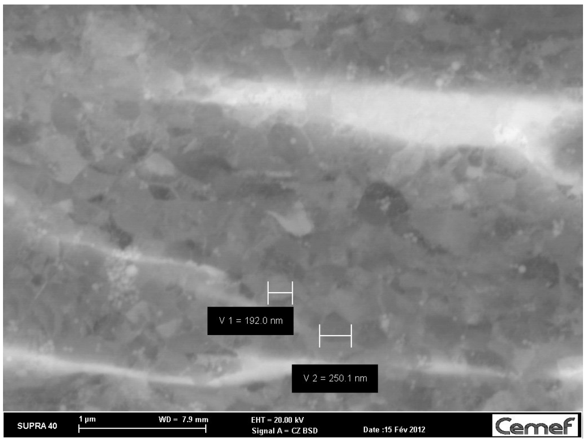

(b) ×20 000

Fig. 5: BSE images of the longitudinal section of the 60% flowformed tube at two different magnification levels

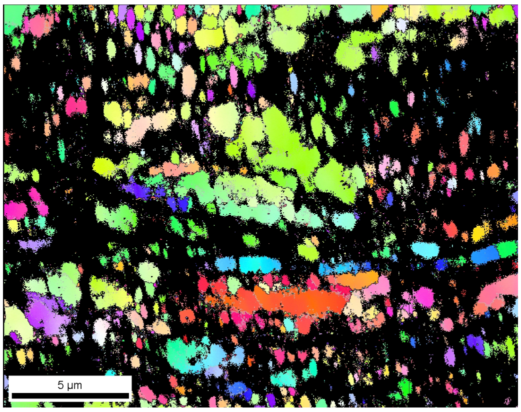

(a) Orientation map for 60% reduction

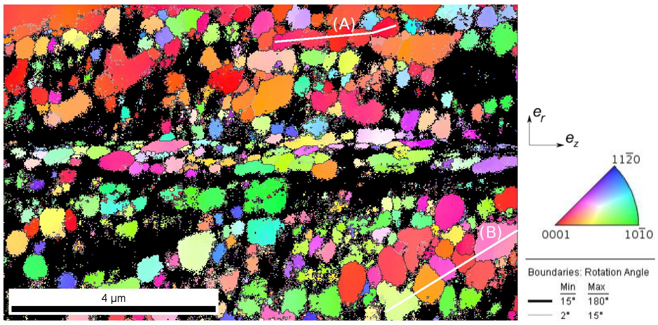

(b) Orientation map for 64% reduction

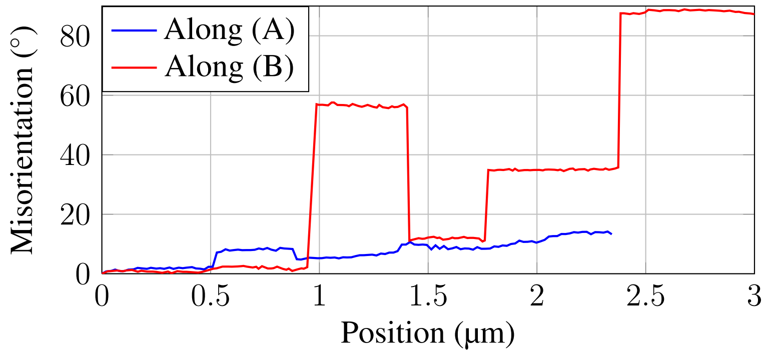

(c) Cumulative misorientation along (A) et (B) on the 64%-flowformed tube

Fig. 6: Results of the EBSD analysis: orientation maps of α phase in the flowformed materials ((a) and (b), longitudinal sections) and misorientation profiles along two lines (c).

Discussion

All recrystallized grains are equiaxed with a uniform size. Furthermore, according to orientation maps (fig. 6) free-dislocation grains appear to be dispersed with a roughly uniform distribution among the high dislocated grains (no necklace-like structure). Those statement tend to indicate that the DRX occurring during flowforming is continuous (CDRX). Hence, it can be related to the so-called CDRX by progressive lattice rotation. Furthermore, titanium alloys have a high stacking fault energy (SFE), which is well known to favour CDRX over discontinuous DRX [23]. As discussed in introduction, DRX is rarely reported in α-β domain on Ti64 using conventional trials, but similar phenomena had been reported in adiabatic shear bands on cold rolled CP titanium [24,25].

The fraction of good points during EBSD analysis for the 60% and 64% -flowformed tubes was 40% and 70%, respectively. Considering that the β phase represents less than 10% in volume, the better indexation for the 64%-flowformed tube indicates that the overall dislocation density in α grains in that tube is lower than in the 60%-flowformed tube, despite its higher strain level. This result can be attributed to either the onset of CDRX, which is known to correspond to a certain critical strain, or the higher forming temperature, due to a higher strain rate. The shape of the grains which display a high intergranular misorientation can not be identified on orientation map, because of non indexed points. But the BSE images (fig. 5) indicate that all (sub-)grains appear roughly equiaxed, thus including high dislocation density grains. This result is opposite of [9,21] who reported that this kind of grains on lamellar structure was severely elongated. Hence, it can be concluded that grains which has not undergone DRX inherit their shape from the prior structure whereas DRXed grains are equiaxed, according to the present work and [9,21].

As stated before, long thin grains with medium dislocation density (I-type) evidenced at moderate strain appear to be replaced by equiaxed grains with low dislocation density and high dislocation density small grains (II and III -types, respectively) at larger strain. As a result, the following scheme could describe the kinetic of grain formation during straining by flowforming:

1. elongation of the prior α grains, governed by slip;
2. breakup of those elongated grains;
3. arrangement and annihilation of the dislocations leading to free-dislocation (sub-)grains (DRV);
4. further rotation of the lattices, creating HAGBs between prior sub-grains (CDRX).

Such grain refinement, as displayed on SEM micrographs, is widely observed on Ti64 constrained to SPD such as equal channel angular extrusion (ECAE), [14,26]. The latter concluded that this refinement was mainly governed by a high twinning activity, which is known to rarely occur on Ti64. In this work, no twin have been evidenced (by SEM observation or EBSD analysis), indicating that the strain was mainly governed by slip.

Thanks to that submicrocristaline structure, the material may have undergone a great amount of mechanical properties, such as yield stress. Furthermore, the relatively low intergranular misorientation, denoting a low dislocation density, revealed by EBSD favours the fatigue resistance and the ductility. The latter indicates that a subsequent forming processing may be possible on the flowformed tubes. A superplastic forming may not be possible yet, due to a low proportion of HAGBs. Nevertheless, the proportion of DRXed grains is still poor, indicating that the DRX is incomplete. Hence, a further strain is probably attainable and it would lead to a complete DRXed structure, with a higher HAGB ratio.

The texture of the α phase can be investigated thanks to EBSD data. The reader may pay attention on the fact that the texture of the non- EBSD-indexed point can not be studied by this means. Furthermore, the scanned area (a few μm^2) is not representative of the entire tubes. Nevertheless, the EBSD analysis provides valuable information about the texture of the recovered grains, as the pole figures resulting from the 64%-flowforming shown on figure 7. According to this figure, the texture shows that the $< c >$ tends to get perpendicular to the tube axis, whereas the $< a >$ component tends to get aligned with that direction. This texture, which is really similar to that of extruded Ti64 [27], is consistent with that reported by [21] on cold flowformed lamellar-structured Ti64. Hence, it suggests that the same phenomenon occurs in both equiaxed and α-colony Ti64 during flowforming. The similarity between flowforming texture and extrusion texture is consistent with the results from the optical microscopy, detailed at the beginning of the present paper.

On the contrary, the last authors have investigated the orientation maps of stress-relieved specimens, without any remarkable "unindexed grains" whereas no subsequent heat treatment has been performed in this present work, leaving some unindexed grains in EBSD analysis. Hence, those parallel studies suggest that the texture of the non-recovered grains is somehow similar to that of recovered. The texture of the 60%-flowformed tube was quite the same as that of the 64%-flowformed (see fig. 7). Thus, the texture of the recovered grains does not seem to change with strain, only the proportion of those grain does (it increases, as stated above). As a result, this texture could be interpreted as the CDRX texture. CDRX has already been reported on magnesium alloy, which is similar to α phase of titanium alloys (hcp structure with a c/a ratio slightly smaller than the ideal value [4], high SFE [28]) by [29]. They investigated the texture of the CDRXed Mg alloy AZ31 and concluded that the basal planes gradually rotate from around 0° to near 90° to the compression axis during CDRX. This texture evolution resulted in a softening during compression, which is rarely reported during CDRX [29,23]. This unusual softening was attributed by the authors to the low CRSS in non-basal slip directions, compared to that of pyramidal slips. As a comparison, the flowforming texture suggests that the stress is mainly compressive in the axial direction during flowforming.

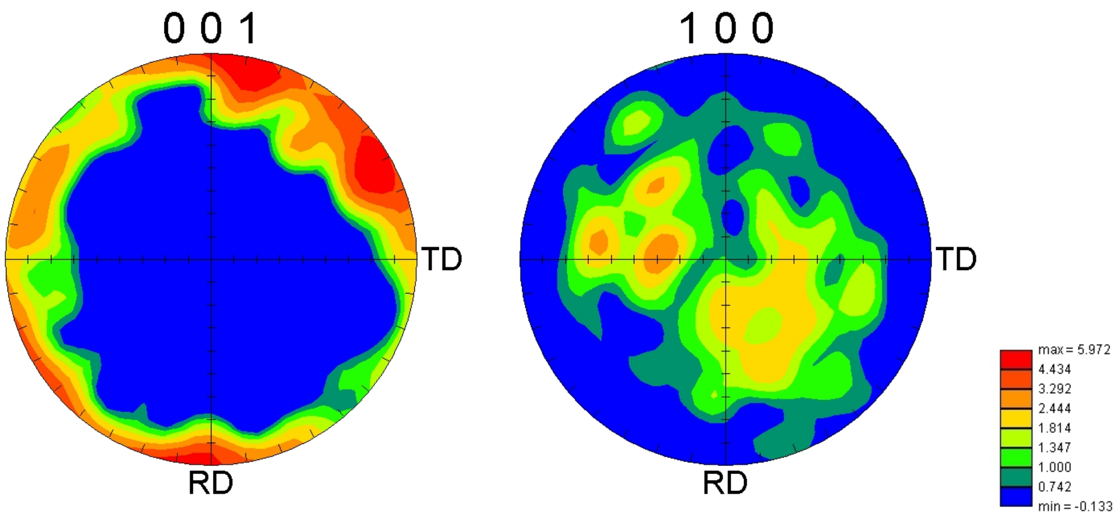

Fig. 7: Pole figures of the α phase in the 64%-flowformed tube. TD and RD denote the through-thickness and the tangential directions, respectively.

The distribution of misorientation angle boundaries in deformed material can be analysed, as reported on figure 8. It denotes a high fraction of LAGBs. Also, one may notice that a higher strain results in a rise of HAGBs, and thus a decrease in LAGBs. This phenomenon can be attributed to a higher lattice rotation level between (sub-)grains, due to higher strain, during CDRX. This misorientation spectrum between α grains is somehow similar to that observed on Ti64 after warm and slow compression ($\dot{\varepsilon} = 10^{-3}\,s^{-1}$ at 800 °C), displaying peaks approximately at 5, 30, 45, 65 and 90° and a large proportion of LAGBs [22]. As the authors of the latter paper did not evidence any DRX, this comparison confirms that DRX encountered during flowfomring is continuous.

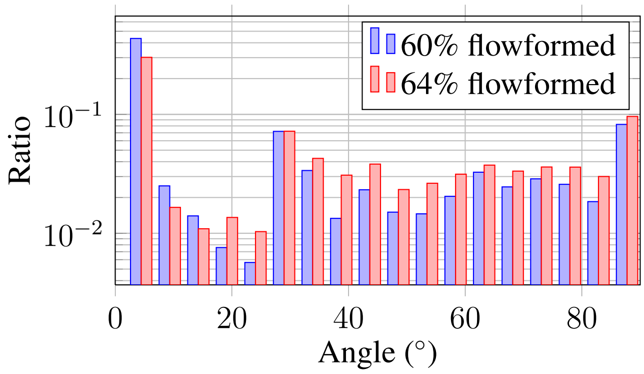

Fig. 8: Distribution of angle misorientation boundaries in deformed material (ordinates in log. scale)

Conclusion

Roughly equiaxed ELI grade Ti-6Al-4V, in tubular shapes, has been highly deformed by cold flow-forming, leading to a reduction in thickness up to 64%. The resulting structures were extensively studied using light optical microscopy, SEM observations and EBSD analysis. The main results of this work are described as following:

- The deformation is mainly longitudinal, making the process really similar to extrusion. The material has been processed out of the conventional stable maps (*i.e.* at high strain rate and low temperature) without any remarkable flow instability such as ASB or cracking. This unusual stability may be due to the cylindrical symmetry.
- At high strain (high reduction in thickness), continuous DRX occurs during flowforming, resulting in equiaxed α grains which can have either a very high dislocation density or a poor dislocation density. The DRX phenomenon was classified as a progressive lattice rotation -type CDRX. This phenomenon allows to severely deform the material without overload on tools nor crack or porosity. At lower strain, DRX is incomplete, leaving some long and thin grains with moderate intragranular misorientations, indicative of moderate dislocation densities.
- The dynamically recovered/recrystallized grains were highly textured, with a $< c >$-axis mainly perpendicular to the tube axis.
- The partial recrystallization observed even on the 64%-flowformed material suggests that a higher reduction in thickness is attainable. It would lead to a high amount of HAGBs.

Acknowledgement

This work was made as part of the Fluoti project, subsidized by the Agence Nationale pour la Recherche (ANR), in collaboration with Timet Savoie, Timet UK Ltd, Roxel France and the CEMEF. The authors are also grateful to Dr. N. Bozzolo and Dr. R. Logé for their advice about the methods and the analysis of the results.

References

[1] Welsch, G. and Bunk, W. May 1982 Metall. Mater. Trans. A 13(5), 889–899.

[2] Zaefferer, S. March 2003 Mat. Sci. Eng. A 344(1-2), 20–30.

[3] Prasad, Y., Seshacharyulu, T., Medeiros, S., and Frazier, W. (2001) J. Mater. Process. Technol. 108(3), 320–327.

[4] Preuss, M., daFonseca, J. Q., Allen, V., Prakash, D. G. L., and Daymond, M. R. July 2010 J. of Strain Anal. for Eng. Des. 45(5), 377 –390.

[5] Santhanam, A. T. and Reed-Hill, R. E. September 1971 Met. Trans. 2, 2619–2622.

[6] Bozzolo, N., Dewobroto, N., Wenk, H. R., and Wagner, F. December 2006 J. of Mat. Sci. 42(7), 2405–2416.

[7] Williams, J., Baggerly, R., and Paton, N. (2002) Metall. Mater. Trans. A 33, 837–850 10.1007/s11661-002-1016-2.

[8] Seshacharyulu, T., Medeiros, S., Frazier, W., and Prasad, Y. February 2002 Mat. Sci. Eng. A 325(12), 112–125.

[9] Gungor, M. N., Ucok, I., Kramer, L. S., Dong, H., Martin, N. R., and Tack, W. T. November 2005 Mat. Sci. Eng. A 410-411(0), 369–374

[10] Seshacharyulu, T., Medeiros, S., Morgan, J., Malas, J., Frazier, W., and Prasad, Y. (2000) Mat. Sci. Eng. A 279(12), 289–299.

[11] Salishchev, G., Galeyev, R., Valiakhmetov, O., Safiullin, R., Lutfullin, R., Senkov, O., Froes, F., and Kaibyshev, O. October 2001 J. Mater. Process. Technol. 116(2-3), 265–268.

[12] Yoshimura, H. and Nakahigashi, J. July 2002 Int J. of Hydrog. Energ. 27(7-8), 769–774

[13] Salishchev, G. A., Valiakhmetov, O. R., and Galeyev, R. M. (1993) J. of Mat. Sci. 28, 2898–2902.

[14] Ko, Y., Lee, C., Shin, D., and Semiatin, S. (2006) Metall. Mater. Trans. A 37, 381–391 10.1007/s11661-006-0008-z.

[15] Ko, Y. G., Lee, C. S., and Shin, D. H. June 2008 Scripta Mater. 58(12), 1094–1097.

[16] Zherebtsov, S., Murzinova, M., Salishchev, G., and Semiatin, S. June 2011 Acta Mater. 59(10), 4138–4150.

[17] Chang, S., Huang, C., Yu, S., Chang, Y., Han, W., Shieh, T., Chung, H., Yao, H., Shyu, G., Hou, H., Wang, C., and Wang, W. August 1998 J. Mater. Process. Technol. 80-81(0), 676–682.

[18] Davidson, M. J., Balasubramanian, K., and Tagore, G. May 2008 J. Mater. Process. Technol. 200(1-3), 283–287

[19] Roy,M., Klassen, R., andWood, J. January 2009 J.Mater. Process. Technol. 209(2), 1018–1025.

[20] Haghshenas, M., Jhaver, M., Klassen, R., and Wood, J. June 2011 Mat. and Des. 32(6), 3629–3636.

[21] Gungor, M. N., Kramer, L. S., Ucok, I., Dong, H., and Tack, W. T. (2007) Flowformed Ti-6Al-4V In Mehmet N. Gungor and Ashraf M. Imam, (ed.), Innovations in Titanium Technology, pp. 37–45 TMS (The Minerals, Metals and Materials Society) Warrendale, PA

[22] Salishchev, G., Zerebtsov, S., Mironov, S., and Semiatin, S. (2004) Formation of grain boundary misorientation spectrum in alpha-beta titanium alloys with lamellar structure under warm and hot working In B Bacroix, JH Driver, R LeGall, C Maurice, R Penelle, H Regle, and L Tabourot, (ed.), Recrystallization and Grain Growth, Pts 1 and 2, volume 467-470, pp. 501–506 Trans Tech Publications Ltd Zurich-Uetikon WOS:000225119800080

[23] Humphreys, F. and Hatherly, M. (2004) Chapter 13 - hot deformation and dynamic restoration In Recrystallization and Related Annealing Phenomena (Second Edition) pp. 415 – V Elsevier Oxford second edition edition.

[24] Yang, Y. and Wang, B. August 2006 Mat. Lett. 60(1718), 2198–2202

[25] Yang, D., An, Y., Cizek, P., and Hodgson, P. May 2011 Mat. Sci. Eng. A 528(12), 3990–3997.

[26] Yapici, G. G., Karaman, I., and Luo, Z.-P. August 2006 Acta Mater. 54(14), 3755–3771.

[27] Coghe, F., Tirry, W., Rabet, L., Schryvers, D., and Van Houtte, P. March 2012 Mat. Sci. Eng. A 537(0), 1–10.

[28] Ravi Kumar, N., Blandin, J., Desrayaud, C., Montheillet, F., and Sury, M. October 2003 Mat. Sci. Eng. A 359(12), 150–157.

[29] Yang, X., Miura, H., and Sakai, T. (2003) Mat. Trans. 44(1), 197203

The Current State-of-the-Art on Material Forming
10.4028/www.scientific.net/KEM.554-557

Submicrocristalline Structure and Dynamic Recovery of Cold Flowformed ELI Grade Ti-6Al-4V
10.4028/www.scientific.net/KEM.554-557.157

View publication stats